CHAPTER VI

Adhesive patches in a poly(ethylene glycol)-matrix reduce bacterial adhesion, while enhancing tissue cell adhesion and macrophage phagocytic activity

Accepted for partial publication in Biomaterials: Wang Y*, Da Silva Domingues JF*, Subbiahdoss G, Van der Mei HC, Busscher HJ, Libera M; **equal contribution*. "Conditions of lateral surface confinement that promote tissue-cell integration and inhibit biofilm growth". *In Press*.

ABSTRACT

Creation of surfaces through which adhesion of bacteria and tissue cells can be controlled for application in biomaterial implants and devices, has hitherto neglected the role of immune cells in this interplay. Here we present a smart patterning of poly(ethylene glycol)-coated glass with adhesive patches by removing the PEG-matrix through e-beam lithography. Adhesive patch diameters and inter-patch distances were varied to yield different adhesive area fractions of glass in a PEG-matrix. Patterns with adhesive patch diameters in the order of 2 – 5 μm separated by distances greater than the patch diameter promoted osteoblast adhesion, spreading and growth and simultaneously reduced staphylococcal colonization. Moreover, macrophages were more efficient in eradicating adhering staphylococci from patterned surfaces than from the PEG-matrix or glass surfaces, because staphylococcal growth was confined to the adhesive patches. This new feature of confined bacterial growth in adhesive patches aided macrophages in their search for adhering bacteria.

INTRODUCTION

Biomaterials play an important role in human life to support and restore function after wear, trauma or surgical intervention in order to create a better quality of life. To this purpose, biomaterials should interact with mammalian cells in a variety of ways, including supporting tissue cell adhesion and integration. However, scientific and clinical communities have long recognized that biomaterial implants and devices provide foreign surfaces, alien to the human body, to which bacteria can adhere and start forming biofilms. Accordingly, biomaterial-associated infection (BAI) is the number one cause of failure of biomaterial implants and devices. Microbial contamination of a biomaterial surface during surgical implantation has been recognized as an important route of contamination, but whether or not microbial contamination eventually results in BAI, depends on the outcome of the so-called "race for the surface" between tissue integration and biofilm formation [1]. If mammalian cells win this race, the implant surface will be covered by a cellular layer and is then less vulnerable to biofilm formation and associated infection. Alternatively, in the inverse case, bacteria will colonize the implant surface and mammalian cell functions are hampered by bacterial virulence factors and excreted toxins [1-3]. BAI is often difficult to treat, as the biofilm mode of growth protects pathogenic microorganisms against both the host defense system and antibiotics [4]. In most cases, the final outcome of BAI is the removal of the implant in order to cure the infection. Consequently, an important challenge facing next-generation biomaterials is to preserve or enhance the ability of a biomaterial implant or device to facilitate tissue integration while simultaneously inhibiting bacterial colonization [1,5].

The pathogenesis of BAI is complex and depends on factors such as the physicochemical properties of the biomaterial surface, virulence of the contaminating bacterial strain, and alterations in the host defense [6]. Following biomaterial implantation, tissue trauma and injury trigger a cascade of events that activate the immune system [7]. Macrophages are one of the most predominant immune cells that arrive within minutes to hours after surgery at an implant site and can remain at a biomaterial surface for several weeks to orchestrate the inflammatory process and foreign body reactions [7-10]. During infection, macrophages detect bacteria via cell surface receptors that bind to bacterial ligands and opsonins [8-10]. Subsequently, macrophages ingest pathogens and activate cellular functions such as proliferation, secretion of proteins and cytokines, and respiratory burst to destroy phagocytized organisms and recruit other cells from the adaptive immune system [8,10]. Therefore, bacteria-biomaterial-immune cell interactions are important factors interfering with the pathogenesis of BAI.

Several surface modifications on biomaterials have been developed to mitigate bacterial colonization, such as poly(ethylene)glycol (PEG) coatings [11-13]. However, while they inhibit bacterial colonization, they simultaneously prevent tissue integration. A surface that differentially promotes interactions with desirable host cells while simultaneously reducing microbial colonization is thus required. Recently, it has been observed that bacterial colonization can be confined to small adhesive patches and that separately growing biofilms in adjacent patches are able to communicate via diffusion of quorum-sensing agents [14-16]. Immune cell response to adhesive patches in a PEG-matrix has never been studied.

In this paper, the influence of adhesive patches in a PEG-matrix on bacterial and mammalian cell adhesion, as well as on macrophage-mediated phagocytosis is explored. In order to identify optimal conditions of lateral surface confinement that

promote mammalian cell adhesion, while inhibiting bacterial adhesion, or alternatively to promote clearance of bacteria from the biomaterial surface by phagocytosis by macrophages, the area of adhesive patches was varied. With a view on a possible orthopedic application, osteoblasts were used as mammalian cells, while *Staphylococcus aureus*, a common pathogen in infections associated with total joint arthroplasties, was taken as a pathogen.

MATERIALS AND METHODS

Surface patterning

Adhesive patches in a poly(ethylene)glycol (PEG)-matrix on glass were prepared using established procedures [17,18]. Briefly, glass slides were sonicated in ethanol (96%), cleaned with a Piranha solution (3:1 of 98% sulfuric acid and 30% H_2O_2) for 30 min, rinsed with deionized water, dried and exposed to low-pressure O2 plasma (300 mTorr, 1.75 W) for 10 min. The slides were then silanized with 2% (v/v) vinyl-methoxy siloxane homopolymer (Gelest Inc.) in ethanol for 10 min, rinsed with deionized water, dried and incubated at 110°C for 2 h. After cooling, thin films of PEG were spin casted onto these substrata using a solution of 2 wt% PEG (6 kDa; Fluka) in tetrahydrofuran. PEG was locally crosslinked with e-beam lithography [19,20]. Spin-coated PEG thin-films were irradiated using a Zeiss Auriga Scanning Electron Microscope (SEM) with a Schottky field-emission electron source (point dose of 10 fC and incident electron energy of 2 keV). The e-beam position and dwell time were controlled using a Nabity Nanometer Pattern Generation System. Subsequently, slides were rinsed in deionized water for 30 min to remove unexposed PEG. The resulting surface consisted of silanized glass patches between surface-bond

patterned PEG thin-film. Arrays patterns were created with a size of 200 × 200 μm on one glass slide, with circular adhesive patches (diameters ranging between 1 and 5 μm) and inter-patch distances between 0.5 and 10 μm. Combinations of different patch diameters and inter-patch distances yielded surfaces with adhesive area fractions (χ) between 0.09 and 0.35, that can be calculated according to

$$\chi = \frac{\pi\left(\frac{\alpha}{2}\right)^2}{(\alpha+\beta)^2} \quad (1)$$

Twelve arrays of 200 × 200 μm were patterned on one glass slide, with the arrays separated from each other by 100 μm wide strips of silanized glass. After patterning, substrata were stored under vacuum (10^{-3} Torr). Light microscopic images of the arrays were taken using a Nikon Eclipse E1000 upright optical microscope. The final thickness of the cross-linked PEG-matrix was determined by atomic force microscopy (AFM, Bruker Bioscope Catalyst).

Fibronectin coating

Fibronectin (Fn) was adsorbed to the patterned slides in some of the experiments, especially to demonstrate the non-adhesiveness of the PEG-matrix with regard to proteins present in serum. Fn was expected to adsorb only to the adhesive patches. Adsorption was performed by immersing the slides in a 25 μg/ml solution of human Fn (Sigma-Aldrich BV) in phosphate buffered saline (PBS: 10 mM potassium phosphate, 0.15 M NaCl, pH 7.0) for 30 min at room temperature and washed three times with sterile PBS. To confirm preferential Fn adsorption on the adhesive patches, a slide was immersed in PBS containing 1% BSA for 1 min to block non-specific protein adsorption, rinsed three times in PBS, exposed to a primary antibody (rabbit-anti-human fibronectin Ab, polyclonal, dilution 1:400 in

PBS) for 30 min, rinsed, and then exposed to a fluorescent secondary antibody (FITC-conjugated donkey-anti-rabbit IgG, dilution 1:100 in PBS). After a final rinse, the patterned glass slide was placed in a Petri dish filled with PBS and examined while fully hydrated by confocal laser scanning microscopy (CLSM, Leica DMRXE with confocal TCS SP2 unit) using a 40x water immersion lens (pinhole was set at its optimal value of 1.0 according to the manufacturer specifications).

Mammalian cell culture conditions and harvesting

Mammalian cells (U2OS osteosarcoma cells) were cultured in Dulbecco's Modified Eagle's Medium (DMEM)-low glucose supplemented with 10% fetal bovine serum (FBS) and 0.2 mM ascorbic acid-2-phosphate (AA2P), denoted as DMEM + FBS. U2OS cells were maintained in tissue culture polystyrene flasks (TCPS, Greiner Bio-One) at 37°C in humidified air with 5% CO2 and harvested at 90% confluence using trypsine / ethylenediamine–tetra-acetic acid. The harvested cells were diluted to 6 x 10^5 cells/ml in DMEM + FBS. U2OS is an immortalized human cell line derived from osteosarcoma cells and was chosen from a broad selection of human osteoblastic cell lines used previously [21]. It has been demonstrated that osteosarcoma cell lines exhibit meaningful osteoblastic phenotypes [22].

U2OS cell adhesion and spreading on Fn-coated, patterned surfaces were studied by *in situ* digital phase-contrast microscopy (Olympus BH-2; 10× objective) in a parallel-plate flow chamber (175 x 17 x 0.75 mm^3) and by *ex situ* immunofluorescence imaging. The flow chamber was equipped with heating elements and maintained at 37°C throughout the experiments. Once fully filled and free of air-bubbles, a U2OS cell suspension was introduced in the flow chamber. The flow was stopped for 1.5 h to allow U2OS cells to settle and adhere to the surface.

Phase-contrast images were taken at this time point from each patterned array and also from areas comprising the PEG-matrix and the glass surface, to determine the initial surface coverage of spread U2OS cells. DMEM + FBS supplemented with 2% HEPES buffer was then perfused through the flow chamber at 0.14 s^{-1} shear rate. After 48 h, the substrata were removed and fixed in 3.7% formaldehyde in cytoskeleton stabilization buffer (CS; 0.1 M Pipes, 1 mM EGTA, 4% (w/v) PEG 8000, pH 6.9). After fixation, samples were incubated in 0.5% Triton X-100 for 3 min, rinsed with PBS, and stained for 30 min with 4 μg/ml of DAPI and 2 μg/ml of TRITC–Phalloidin. Slides were examined by fluorescence microscopy (Leica DM4000B). The total surface coverage of adhering cells on the patterned surfaces was determined by Scion image software. The surface coverage by U2OS cells during the spreading period was defined as

$$\Phi = \frac{\phi_{48} - \phi_{1.5}}{\phi_{1.5}} \qquad (2)$$

where ϕi was the area fraction of surface covered by U2OS cells after 1.5 or 48 h. A positive value of Φ indicated that the cells spread on the surface and might be proliferating, while a negative value of Φ indicated that the cells either contracted or, more likely, migrated off the patterned surface. Each data point corresponds to average and standard deviation from three different experiments with three independent U2OS cell cultures.

Bacterial culture conditions and harvesting

S. aureus NCTC 8325-4 were provided by T. J. Foster (Moyne Institute of Preventive Medicine, Dublin, Ireland). This strain possesses Fn-binding proteins. Bacteria were inoculated on trypsine soy broth (TSB, Oxoid) agar plates and incubated overnight at 37°C. One colony was grown in 10 mL TSB overnight with

constant rotation (120 rpm) and subsequently used to inoculate 190 ml TSB. Approximately after 2 h of incubation, *S. aureus* NCTC 8325-4 was in its exponential phase of growth with the peak of Fn-binding protein expression, bacteria were harvested by centrifugation (5,000 g, 5 min, 10°C) and washed twice in sterile PBS. Bacterial aggregates were broken by mild, intermittent sonication on ice (3 times, 10 s, 30 W, Wibra Cell model 375, Sonics and Materials Inc., Danbury, Connecticut, USA) and re-suspended to a concentration of 3×10^8 bacteria/ml in PBS. Bacterial adhesion to Fn-coated, patterned surfaces were studied in a parallel-plate flow chamber and monitored *in situ* by digital phase-contrast microscopy. After removing air bubbles from the tubing by flowing PBS, the *S. aureus* suspension was perfused through the chamber (shear rate of 11 s^{-1}) for 30 min at room temperature. After bacterial deposition, sterile PBS was flowed through the system for 30 min to remove non-adhering bacterial from the chamber and tubing system. TSB was then flowed through the system at a low shear rate (0.14 s^{-1}) for 24 h. A heating element maintained the chamber temperature at 37°C. After 24 h, another 30 min of PBS washing (shear rate 11 s^{-1}) was performed. All experiments were done in triplicate with three independent bacterial cultures. Phase-contrast images were taken during the bacterial growth from each patterned array and from surrounding PEG-matrix and glass surface at 1 min time intervals. The number of adhering bacteria per unit area on each array, the PEG-matrix and the glass surface was quantified at different time points, using proprietary software based on the Matlab Image processing Toolkit (The MathWorks, Natick, MA, USA).

Macrophages culture conditions and harvesting

A murine macrophage cell line (J774A.1; ATCC TIB-67) was used in this study. Macrophages were routinely cultured in DMEM supplemented with 4.5 g/l

D-glucose, pyruvate and 10% FBS containing Fn (referred as DMEM-HG + FBS), in TCPS. The TCPS flasks were maintained at 37°C in a humidified atmosphere with 5% CO_2 and cells were passaged at 70 – 80% confluence by scraping. Cells were harvested by centrifugation (5 min at 150 x g) in DMEM-HG + FBS previous to experiments. Harvested cells were set to a concentration of 6 x 10^6 cells/ml in DMEM-HG + FBS. Macrophage interactions with *S. aureus* NCTC 8325-4 on patterned surfaces with different adhesive patch diameters and inter-patch distances, including a completely PEG-coated surface and a completely silanized glass surface, were studied by *in situ* imaging in the parallel-plate flow chamber. Two different sets of patterned glass slides were prepared for this experiment. After biofilm growth for 1 h according to the protocol described above, the entire volume of TSB inside the chamber was replaced by DMEM-HG + FBS, to remove the non-adhering bacteria from the tubes and chamber. Subsequently, the macrophage suspension was inserted into the flow chamber. Once the entire volume of DMEM-HG + FBS inside the chamber was replaced by the macrophage suspension, the flow was stopped in order to allow macrophages to adhere to the surface. Subsequently, macrophage-bacteria interactions were followed for 2 h in static conditions. The number of bacteria that had remained adhering after phagocytosis was determined using proprietary software based on the Matlab Image processing Toolkit (The MathWorks), and subtracted from the number of bacteria adhering before insertion of macrophages. By normalizing this difference with respect to the number of staphylococci initially adhering and the time allowed for phagocytosis, phagocytosis rates were obtained, as previously outlined in detail [23]. All experiments were done in triplicate with separately grown bacterial and macrophage cell cultures.

RESULTS

Patterned surfaces

Circular adhesive patches in a PEG-matrix (Figure 1) were prepared on silanized glass arranged in a square array and coated with fibronectin (Fn), one of the main proteins in serum (see Figure 1E, F). Fn adsorption is clearly confined to the adhesive patches and not occurring on the PEG-matrix surrounding the patches. Figures 1C, D show an AFM topographic image (tapping mode) with a graph profiling the height along several adjacent patches, respectively. The dry height of the PEG-matrix surrounding each patch is approximately 80 nm. These e-beam patterned PEG-matrix swells by a factor of approximately 1.5 to 3 when hydrated [17,19].

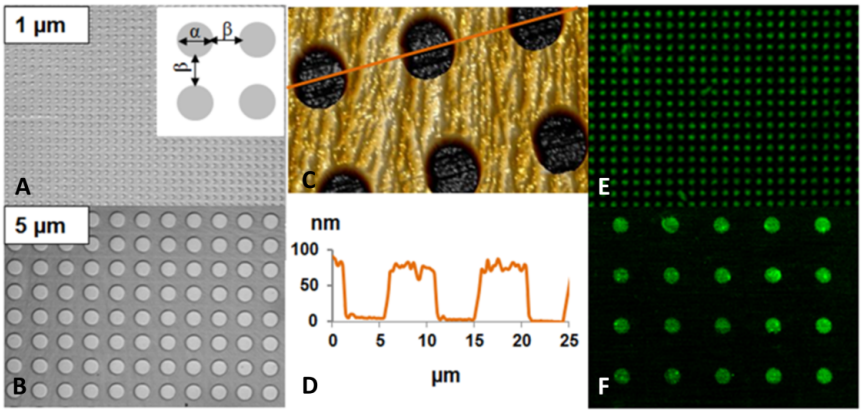

Figure 1. Examples of adhesive patches in a PEG-matrix. (A) and (B) phase-contrast microscopy images of patches with an adhesive area fraction, χ, of 0.35; (C) and (D) AFM image with a height profile from a dry patterned film with α = 5 µm and χ = 0.20; (E) and (F) CLSM snapshots showing Fn adsorption (green) onto the adhesive patches for surfaces with an adhesive area fraction of 0.09.

Mammalian cell interactions

Mammalian cells (U2OS osteoblasts) were cultured on PEG-patterned surfaces in a parallel-plate flow chamber to evaluate their interaction with these surfaces. For this purpose, different combinations of adhesive patch diameters and inter-patch distances were prepared in a PEG-matrix. In Figure 2 the morphology of U2OS cells is shown as a function of the patch diameter (α) and inter-patch distance (β). Initial adhesion and spreading after 1.5 h of seeding was similar on all differently patterned surfaces. The immunofluorescence images show that the cells effectively spread after 48 h on the surfaces with 3 and 5 μm diameter adhesive patches. Adhesion and spreading decreased with decreasing patch diameter. For a patch diameter α = 1 μm, it was observed that the cells effectively migrated away from the patterned surface onto the adjacent, fully adhesive surface.

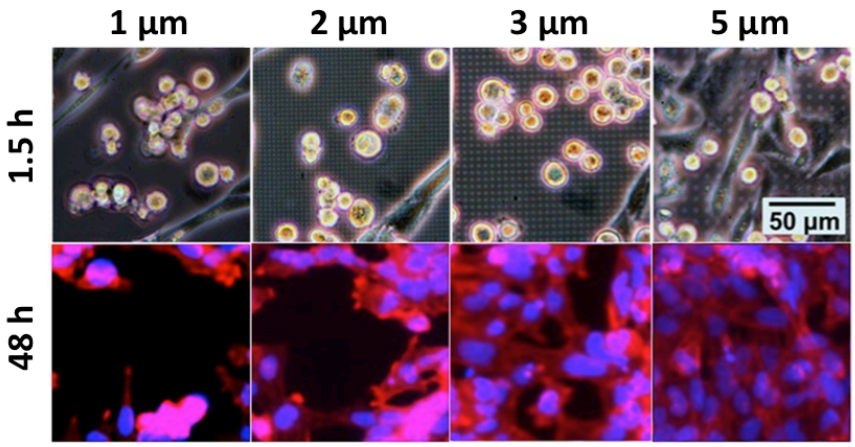

Figure 2. Phase-contrast images (top row) and immunofluorescence images (bottom row) of U2OS cells interacting with different adhesive patches in a PEG-matrix. Images represent an example of U2OS cells interacting with surfaces of different patch diameter α (1, 2, 3 and 5 μm) and a constant adhesive area fraction of χ = 0.20. Phase-contrast images were taken after 1.5 h adhesion of U2OS cells and immunofluorescence images after 48 h of seeding.

The surface coverage by U2OS cells for different area fractions of the adhesive patches *versus* the PEG-matrix is presented in Figure 3A for 1.5 h after seeding. At this early time point, spreading still is limited on all surfaces as shown by the similar coverage, although coverage was lowest for an adhesive patch diameter of 1 μm. After 48 h of cell spreading, differences were much more pronounced. The fractional change in cell surface coverage (Figure 3B) indicates that this is due to cell spreading rather than cell growth, since under the chosen culture conditions U2OS cells typically start proliferating after 48 h [19]. The largest coverage was observed for the surfaces with adhesive patches of 5 μm diameter, regardless of the inter-patch distance and resulting adhesive area fraction. In contrast, adhesive patches of 1 μm diameter revealed no spreading, implying that the U2OS cells migrated off the patterned surface.

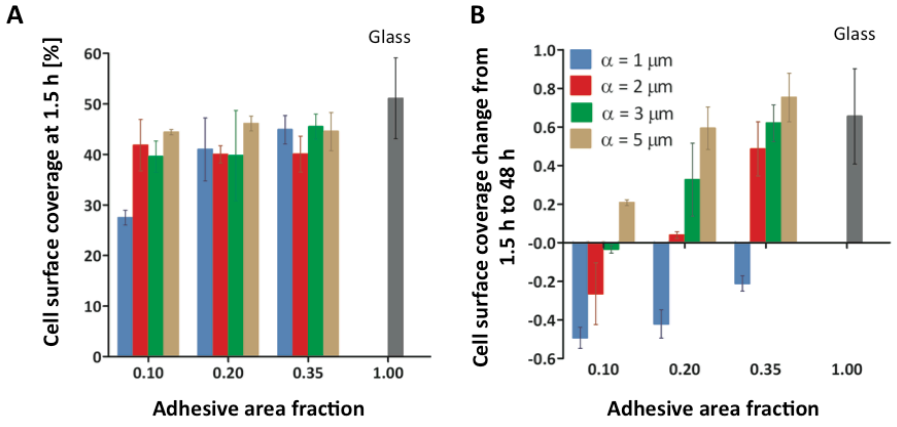

Figure 3. Quantification of U2OS cell surface coverage on adhesive patches in a PEG-matrix for different adhesive area fractions. (A) U2OS cell surface coverage after 1.5 h; (B) fractional change in cell surface coverage from 1.5 h to 48 h with respect to the fraction of surface covered by U2OS cells after 1.5 h for different diameters α of the adhesive patches. All data is represented as average and standard deviation over three different experiments with separately cultured cells.

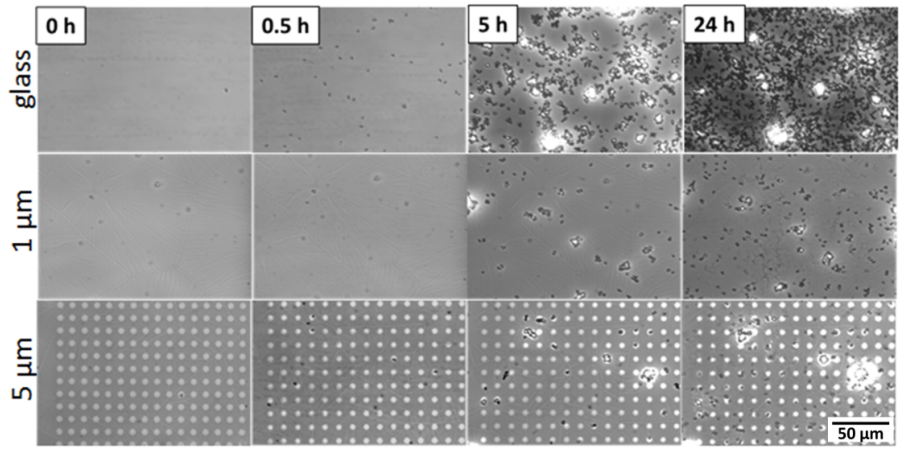

Figure 4. Representative time-resolved phase-contrast images of *S. aureus* NCTC 8325-4 adhesion and growth. Images show the adhesion (t = 0 – 0.5 h) and growth (t = 5 h and t = 24 h) of *S. aureus* on unpatterned glass (top row) and patterned surfaces with an adhesive area fraction χ = 0.2 with an adhesive patch diameter of 1 µm (middle row) or 5 µm (bottom row).

Bacterial adhesion and growth

Bacterial adhesion and growth on PEG-patterned surfaces was studied in a parallel-plate flow chamber. Representative phase-contrast images from time-lapse recordings of *S. aureus* NCTC 8325-4 colonization of surfaces with different adhesive patches are shown in Figure 4. After 24 h of growth, the unpatterned silanized glass surface was heavily populated by bacteria. In contrast, far less bacteria were present on the patterned surfaces. Interestingly, 5 µm diameter adhesive patches in a PEG-matrix showed several 3-D colonies whose size exceeded the diameter of the adhesive patches. All patterns reduced the initial adhesion of *S. aureus* NCTC 8325-4 (Figure 5A), when compared with the unpatterned glass, by one order of magnitude or more. Bacterial growth (Figure 5B) was only quantified after 5 h, since longer growth periods resulted into multi-layered bacteria, which could not be quantified with the microscopic technique applied. Also after growth, staphylococcal

numbers were reduced on patterned surfaces when compared to their initial numbers on unpatterned glass.

The growth rates of individual *S. aureus* adhering on the differently patterned surfaces are summarized in Figure 6, as expressed as the number of staphylococci within individual adhesive patches. When unconstrained, a bacterium underwent approximately 5 doubling cycles, over the subsequent 5 h of growth following initial adhesion, to form a cluster of approximately 30 bacteria. For the patterned surfaces a single bacterium grew to 5 bacteria for the 5 μm and 2 – 3 bacteria for 3 μm diameter adhesive patches. In 2 μm adhesive patches, we did not observe any growth of adhering staphylococci.

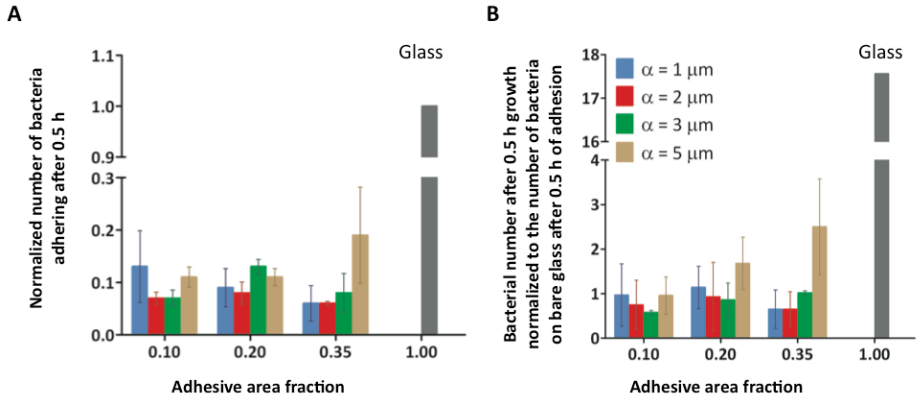

Figure 5. Quantification of staphylococcal adhesion and growth on surfaces with different adhesive area fractions and patch diameters. (A) Number of adhering *S. aureus* after 0.5 h deposition normalized with respect to the number of adhering bacteria on glass ((6.8 ± 1.1) x 10^5 cm^{-2}); (B) Number of adhering *S. aureus* after 5 h growth normalized to the initial number of adhering bacteria on glass ((6.8 ± 1.1) x 10^5 cm^{-2}). All data is represented as average and standard deviation over three different experiments with separately cultured bacteria.

Macrophage-Mediated Phagocytosis on Patterned Substrata

In order to study the interactions between bacteria and macrophages on PEG-patterned surfaces, bacteria were first adhered to PEG-patterned surfaces under flow conditions prior to adding macrophages, mimicking the situation of perioperative bacterial contamination of implant surfaces [24]. In Figure 7, the number of adhering staphylococci on patterned surfaces is shown after initial adhesion (30 min), after subsequent bacterial growth (30 – 90 min) and after macrophage-mediated phagocytosis (90 – 210 min). After 30 min of bacterial adhesion, lowest and highest numbers of adhering staphylococci were found on the PEG-matrix and on the glass surface respectively, with intermediate numbers of bacteria on the differently patterned surfaces. After 1 h of biofilm growth (t = 90 min), an increase in the number of bacteria was observed on all surfaces, with the highest number of staphylococci found on glass. The number of macrophages also showed extremes on the PEG-matrix (2.0×10^4 cm^{-2}) *versus* glass (5.0×10^4 cm^{-2}), while on patterned surfaces macrophages adhered in similar numbers as on the PEG-matrix (2.5×10^4 cm^{-2}). After bacterial-macrophage interaction for 2 h (t = 90 – 210 min), a decrease in the number of adhering *S. aureus* was observed due to macrophage-mediated bacterial phagocytosis (see Figure 7) on all surfaces. From the decrease in the number of *S. aureus* NCTC 8325-4 and the number of macrophages present, the number of staphylococci engulfed by a single macrophage per unit time can be calculated, also referred to as the "phagocytosis rate" [23]. Phagocytosis rates were similar on the differently patterned surfaces (ranging from $(0.9 \pm 1.0) \times 10^{-7}$ to $(1.5 \pm 1.8) \times 10^{-7}$ cm^2/min) regardless of the diameter of the adhesive patches and the adhesive area fraction. On glass and on the PEG-matrix, bacteria were phagocytized from the surface at slower rates of $(0.05 \pm 0.4) \times 10^{-7}$ and $(0.2 \pm 0.6) \times 10^{-7}$ cm^2/min, respectively.

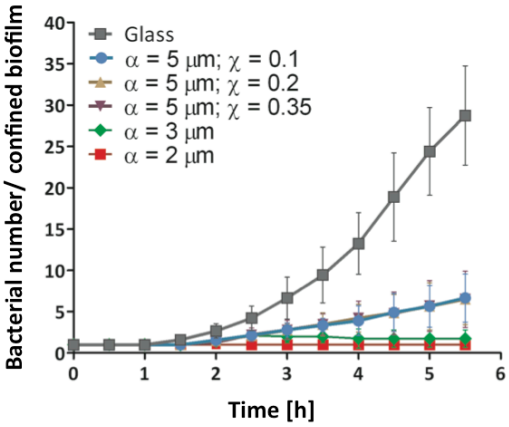

Figure 6. The number of *S. aureus* within individual adhesive patches as a function of time after initial adhesion for different diameters α of the adhesive patches and adhesive area fractions χ. Each data point corresponds to the average and standard deviation of at least 20 different patches on each surface. Bacteria on 1 μm diameter adhesive patches could not followed, because it was impossible to resolve the adhesive patches with the microscope settings used for imaging.

DISCUSSION

There has been a great interest over the past decade in creating surfaces through which adhesion of bacteria and tissue cells can be controlled, especially in the development of infection-resistant biomaterials for tissue-integratable implants and devices [11-13], but the role of immune cells has been largely neglected in this interplay. The most common approach is to define regions that resist or promote respectively, the adhesion of bacteria and mammalian cells by patterning hydrophilic and hydrophobic regions on the surface [19,20,25]. In our study, surfaces were produced with circular patches of adhesion promoting silanized glass separated by an adhesion resistant, hydrophilic PEG-matrix. On such surfaces, staphylococcal adhesion and growth were confined to the adhesive patches, while mammalian cells

were able to adhere and spread on the different PEG-patterned surfaces. Interestingly, macrophage-mediated phagocytosis of adhering staphylococci was more efficient on PEG-patterned surfaces than on the unpatterned glass or on the PEG-matrix.

Bacterial adhesion by flow-mediated deposition, on the differently designed PEG-patterned surfaces, appeared to be largely independent of the adhesive patch diameter. In theory, bacteria that were close to the surface should adhere within a finite window of time and dependent on the flow rate and the size of the adhesive patch. However, in this experimental design the chosen different patch diameters do not seem to be discriminative with respect to numbers of adhering organisms.

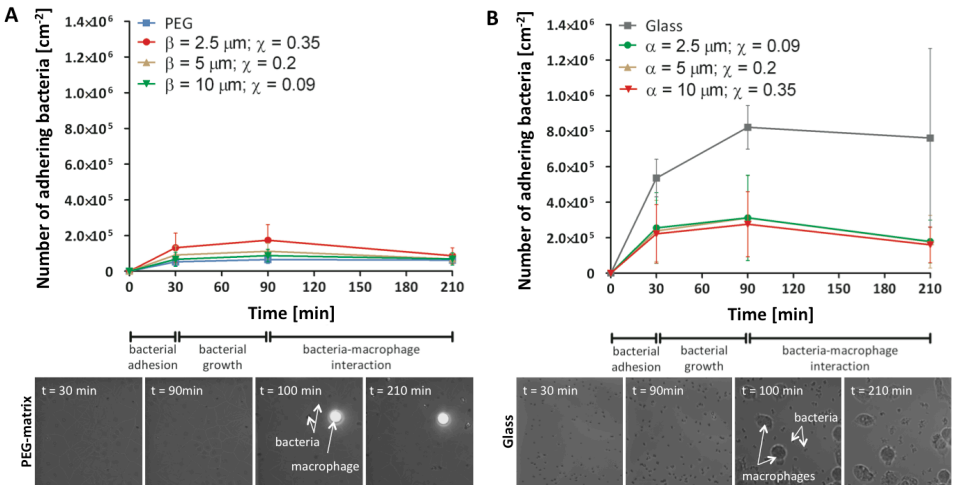

Figure 7. Number of adhering *S. aureus* NCTC 8325-4 on patterned surfaces with different distances β between adhesive patches and adhesive patch diameters α, yielding different adhesive area fractions χ, as a function of time after initial adhesion, growth and interaction with macrophages. Examples of phase contrast images of the unpatterned surfaces at different time points are shown below each graph. (A) Numbers of adhering staphylococci on patterned surfaces with an adhesive patch diameter α of 5 μm and different inter-patch distances β, and on unpatterned PEG-matrix surfaces; (B) Numbers of adhering staphylococci on patterned surfaces with an inter-patch distance β of 5 μm and different adhesive patch diameters α, and on unpatterned glass surfaces. All data is represented as average and standard deviation over three different experiments with separately cultured bacteria and macrophages.

Differences in colonization became visible though through confined growth in the adhesive patches and solely in the case of patterns with a diameter α = 5 μm and an inter-patch distance β = 2.5 μm, staphylococci were able to bridge the non-adhesive PEG-matrix. Therefore, a minimum inter-patch distance is critical in order to retain confined growth. Results suggest that the development of a growing bacterial biofilm into a mature biofilm can be delayed or inhibited by spatial confinement. If biofilm formation is arrested on such surfaces, the development of hierarchical biofilm structures and varying bacterial phenotypes may also be impeded. On the other hand, confinement of actively growing biofilms did not prevent the release of planktonic daughter cells and adhesion to the surface. Data show that surface confinement had a substantial impact on the bacterial growth and that biomaterial surfaces can be structured in order to reduce bacterial colonization.

The differently patterned surfaces revealed that there is a minimum adhesive area needed for U2OS cell adhesion and spreading. Contrary to other studies [25], where fibroblasts were shown to adhere and spread on adhesive patches with diameters as small as 100 nm and surrounded by a PEG-matrix, in our study U2OS cells were unable to adhere and spread on patterns with adhesive patches of 1 μm diameter. The effects of matrix topography may hinder cell adhesion when the adhesive patch size becomes too small, the critical size of which may differ per cell type. The PEG-matrix separating the adhesive patches was approximately 120 nm thick when hydrated. In order for a cell to bridge the PEG-matrix in between two adjacent adhesive patches, cells probably have to generate a certain membrane curvature at the edge of each patch. The radius of curvature has to increase when the patch size decreases, which may be limiting for further cell adhesion and spreading.

Macrophages play an important role in both inflammation and infection, but often in BAI, macrophages are hampered in eradicating infecting bacteria [25-27].

To clear bacteria in a biofilm mode of growth from a biomaterial surface, macrophages need to break the adhesive bonds between bacteria and between bacteria and a substratum surface. Bacteria and macrophages are known to adhere strongly to glass and only weakly to PEG coated surfaces [24,25]. Due to strong attachment, macrophages on glass do not migrate to engulf bacteria as much as they do on the PEG-matrix and accordingly, lower phagocytosis rates were observed on the glass surface than on the PEG-matrix. As a consequence of the stronger adhesion forces experienced by macrophages on glass, macrophages tend to move to the unpatterned glass surrounding the patterns, but this is merely a result of the experimental design chosen in which multiple patterns were created on a single glass slide. Möller *et al.* [27] have shown that macrophages use small cellular projections (filopodia) to sense the surrounding microenvironment in search for bacteria. Filopodia can be very fast in finding bacteria [24], which explains why macrophages were more effective in eradicating bacteria from patterned surfaces, on which bacteria were adhering in the confinement of the adhesive patch.

CONCLUSION

Smartly patterning the surfaces of a tissue-contacting biomaterial implants and devices may be useful for promoting healing and reducing the risk of BAI. For a clinical application, our results suggest that there is a window of surfaces with adhesive patches in the order of 2 – 5 μm separated by distances greater than the patch diameter that can promote osteoblast adhesion, spreading and growth and simultaneously reduce staphylococcal colonization. Moreover, macrophages are more efficient in eradicating adhering staphylococci from adhesive patches, confined by a PEG-matrix than from glass surfaces or the PEG-matrix itself.

REFERENCES

1. Gristina AG (1987) Biomaterial-centered infection: microbial adhesion *versus* tissue integration. *Science* 237: 1588-1595.
2. Song Z, Borgwardt L, Høiby N, Wu H, Sørensen TS, *et al.* (2013) Prosthesis infections after orthopedic joint replacement: the possible role of bacterial biofilms. *Orthop Rev (Pavia)* 5: 65-71.
3. Costerton JW, Montanaro L, Arciola CR (2007) Bacterial communications in implant infections: a target for an intelligence war. *Int J Artif Organs* 30: 757-763.
4. Trampuz A, Zimmerli W (2005) New strategies for the treatment of infections associated with prosthetic joints. *Curr Opin Investig Drugs* 6: 185-190.
5. Busscher HJ, Van der Mei HC, Subbiahdoss G, Jutte PC, Van den Dungen JJ, *et al.* (2012) Biomaterial-associated infection: locating the finish line in the race for the surface. *Sci Transl Med* 4: 153rv10.
6. Boelens JJ, Dankert J, Murk JL, Weening JJ, Van der Poll T, *et al.* (2000) Biomaterial-associated persistence of *Staphylococcus epidermidis* in pericatheter macrophages. *J Infect Dis* 181: 1337-1349.
7. Anderson JM (2004) Inflammation, wound healing, and the foreign-body response. In: Ratner BD, Hoffman AS, Schoen FJ, Lemons JE, editors. *Biomaterials Science. An Introduction to Materials in Medicine.* Elsevier, San Diego, CA. pp 296-304.
8. Aderem A, Underhill DM (1999) Mechanisms of phagocytosis in macrophages. *Annu Rev Immunol* 17: 593-623.
9. Underhill DM, Ozinsky A (2002) Phagocytosis of microbes: complexity in action. *Annu Rev Immunol* 20: 825-852.
10. Stuart LM, Ezekowitz RAB (2005) Phagocytosis: elegant complexity. *Immunity* 22: 539-550.
11. Hucknall A, Simnick AJ, Hill RT, Chilkoti A, Garcia A, *et al.* (2009) Versatile synthesis and micropatterning of nonfouling polymer brushes on the wafer scale. *Biointerphases* 4: FA50-7.
12. Lichter JA, Rubner MF (2009) Polyelectrolyte multilayers with intrinsic antimicrobial functionality: the importance of mobile polycations. *Langmuir* 25: 7686-7694.
13. Magin CM, Long CJ, Cooper SP, Ista LK, López GP, *et al.* (2010) Engineered antifouling microtopographies: the role of Reynolds number in a model that predicts attachment of zoospores of *Ulva* and cells of *Cobetia marina*. *Biofouling* 26: 719-727.
14. Carnes EC, Lopez DM, Donegan NP, Cheung A, Gresham H, *et al.* (2010) Confinement-induced quorum sensing of individual *Staphylococcus aureus* bacteria. *Nat. Chem Biol* 6: 41-45.
15. J Boedicker JQ, Vincent ME, Ismagilov RF (2009) Microfluidic confinement of single cells of bacteria in small volumes initiates high-density behavior of quorum sensing and growth and reveals its variability. *Angew Chem Int Ed Engl* 48: 5908-5911.
16. Vincent ME, Liu W, Haney EB, Ismagilov RF (2010) Microfluidic stochastic confinement enhances analysis of rare cells by isolating cells and creating high density environments for control of diffusible signals. *Chem Soc Rev* 39: 974-984.

17. Krsko P, Saaem I, Clancy R, Geller H, Soteropoulos P, Libera M (2005) E-beam patterned hydrogels to control nanoscale surface bioactivity. In: Lai WY, Ocola LE, Pau S, editors. *Nanofabrication: Technologies, Devices, and Applications II*. SPIE; Bellingham. pp 600201.

18. Krsko P, Mansfield M, Sukhishvili S, Clancy R, Libera M (2003) Electron-beam patterned poly(ethylene glycol) microhydrogels. *Langmuir*, 19: 5618-5625.

19. Wang Y, Subbiahdoss G, Swartjes J, Van der Mei HC, Busscher HJ, *et al.* (2011) Length-scale mediated differential adhesion of mammalian cells and microbes. *Adv. Funct. Mater.* 21: 3916-3923.

20. Dai X, Yang W, Firlar E, Marras SAE, Libera M (2012) Surface-patterned microgel-tethered molecular beacons. *Soft Matter* 8: 3067-3076.

21. De Ruijter JE, Ter Brugge PJ, Dieudonne SC, Van Vliet SJ, Torensma R, *et al.* (2001) Analysis of integrin expression in U2OS cells cultured on various calcium phosphate ceramic substrates. *Tissue Eng* 7: 279-289.

22. Clover J, Gowen M (1994) Are MG-63 and HOS TE85 human osteosarcoma cell lines representative models of the osteoblastic phenotype? *Bone* 15, 585-591.

23. Da Silva Domingues JF, Van der Mei HC, Busscher HJ, Van Kooten TG (2013) Phagocytosis of bacteria adhering to a biomaterial surface in a surface thermodynamic perspective. *PLoS One* 8: e70046.

24. Saldarriaga Fernández IC, Da Silva Domingues JF, Van Kooten TG, Metzger S, Grainger DW, *et al.* (2011) Macrophage response to staphylococcal biofilms on crosslinked poly(ethylene) glycol polymer coatings and common biomaterials *in vitro*. *Eur Cell Mater* 21: 73-79.

25. Koh WG, Revzin A, Simonian A, Reeves T, Pishko M (2003) Control of mammalian cell and bacteria adhesion on substrates micropatterned with poly(ethylene glycol) hydrogels. *Biomed Microdev* 5: 11-19.

26. Miller M, Dreisbach A, Otto A, Becher D, Bernhardt J, *et al.* (2011) Mapping of interactions between human macrophages and *Staphylococcus aureus* reveals an involvement of MAP kinase signaling in the host defense. *J Proteome Res* 10: 4018-4032.

27. Möller J, Lühmann T, Chabria M, Hall H, Vogel V (2013) Macrophages lift off surface-bound bacteria using a filopodium-lamellipodium hook-and-shovel mechanism. *Sci Rep* 3: 2884.